Available online at www.eccomasproceedia.org
Eccomas Proceedia COMPDYN (2021) 3021-3035

ECCOMAS Proceedia

COMPDYN 2021
8th ECCOMAS Thematic Conference on
Computational Methods in Structural Dynamics and Earthquake Engineering
M. Papadrakakis, M. Fragiadakis (eds.)
Streamed from Athens, Greece, 28 - 30 June 2021

PASSIVE CONTROL ISSUES ON THE LONGITUDINAL AND TRANSVERSE VIBRATIONS OF FLEXIBLE PYLONS

George D. Manolis[1], **and George I. Dadoulis**[2]

[1] Department of Civil Engineering
Aristotle University, Thessaloniki 54124, Greece
e-mail: gdm@civil.auth.gr

[2] Department of Civil Engineering
Aristotle University, Thessaloniki 54124, Greece
gdadoulis@civil.auth.gr

Abstract

The influence of passive mass dampers and base isolators on the vibratory motion of flexible beams with uniform cross-section, viewed as a special case of the non-uniform one, is examined herein for both axial and flexural vibrations. Use of such beams is widespread, both in a mechanical engineering setup (e.g., wind turbines, aircraft blades) as well as in a civil engineering setup (e.g. pylons, antennas). We start with an analytical solution to the governing equations of motion to recover the eigenproperties of a cantilevered pylon in the presence of a top mass and base springs. This is followed by the complete solution for the case of harmonic ground motion using modal analysis. Results are finally presented in term of transmissibility functions, defined as the ratio of the top pylon displacement amplitude to that of the base motion, so as to identify the frequency range where the presence of these external control devices is beneficial.

Keywords: Pylons, Flexible Structures, Vibrations, Passive Control, Elastic Waveguides, Lumped Mass, Soil Springs

ISSN:2623-3347 © 2021 The Authors. Published by Eccomas Proceedia.
Peer-review under responsibility of the organizing committee of COMPDYN 2021.
doi: 10.7712/120121.8693.19669

1 INTRODUCTION

The kinematic and stress fields that develop in elastic beams are dependent on the material properties, the geometry and on the external loads. For dynamic loads, retaining a continuous distribution of the mass of the beam along its length yields an elastic waveguide [1,2] that can exhibit flexural, axial and torsional vibrations. Beams in flexure with a non-uniform cross-section are governed by a fourth order, linear partial differential equation (PDE) with variable coefficients, while for the other two modes of vibration the equations of motion are PDE of second order. It is also possible to have coupling between the axial and flexural vibrations, which requires solution of two coupled PDE. Furthermore, if a lumped mass is placed at the top of the beam, or if its foundation is elastic, then the boundary conditions change and are no longer homogeneous. These two additions modify the structural response of the beam and their presence can be viewed as a means of passive structural control. A discussion of the circumstances under which the effects of rotatory inertia and shear deformation must be considered, and whether or not coupling of flexural and axial vibrations is important, have be found elsewhere [3,4]. In general, for flexible pylons serving as part of power transmission lines and as telecommunication antennas, and for the frequency range of ambient vibrations generated by traffic, the aforementioned effects seem to be of minor importance. We note that this frequency range is roughly *20-200 Hz*, with flexural vibrations occurring in the lower part and axial vibrations in the higher part of the spectrum. On the other hand, the Bernoulli-Euler beam theory fails and has to be upgraded to Rayleigh's model with the rotatory inertia of the cross-section included in the equations of motion, for high vibration frequencies in excess of *500 Hz*.

The literature is rich in the solution of continuous beams under dynamic loads [5], but research interest remains strong, because these elements play a pivotal role in structural engineering (e.g., column elements) and in mechanical engineering (e.g., blades). In the interest of brevity, we simply mention here a recent paper [6] on an exhaustive analysis of wind turbines in an offshore environment under all three response modes (bending, compression, torsion) to a variety of environmentally-induced loads. From our perspective, the field of application of this work, which is continuation of a previous publication [4], is structural health monitoring (SHM). More specifically, modern advances in hardware have rendered possible the use of wireless sensors that send signals to a central processing unit, which in turn evaluates them to decide if the integrity of the structure in question has been compromised [7,8]. To stem the flow of large data over time, it is essential that these sensors be equipped with software based on reliable and efficient numerical models representing the structure in question. This way, computations can be carried out locally to produce results against which the recorded signals may be compared. This allows for a first evaluation of the recorded data, which can be discarded if it just shows a routine response of the structure to ambient vibrations. Furthermore, an SHM system can be placed within an artificial intelligence (AI) environment [9], which would serve to monitor the structural response in the absence of an overseer and give alert signals when it becomes evident that the structure in question is experiencing duress due to environmentally induced loads and needs to be inspected.

In here, we examine simple methods for passive vibration protection of a cantilevered pylon used as part of an electric transmission line for railways by formulating the equations of motion for flexural and axial vibrations. The pylon is then augmented with either of two elementary passive structural control devices, namely a lumped mass at the top and a base isolator in the form of springs at the base. The magnitude of the lumped mass has to be relatively small compared to the total mass of the pylon so as to serve as a secondary system [10] whose fixed-base natural frequency can be tuned with respect to the eigenfrequencies of the pylon.

2. MATHEMATICAL MODELS FOR NON-UNIFORM BEAMS

We will formulate the mathematical models for the tapered cantilevered pylon shown in Fig.1, where placement of a lumped mass at the top and of springs at the base serve as rudimentary passive damping devices. Then, the uniform cross-section cantilevered pylon can be recovered as a special case. By considering in Fig. 1 the force and moment equilibrium of a differential segment dx under distributed longitudinal $p(x,t)$ and transverse $f(x,t)$ loads, we obtain the coupled governing equations of motion as

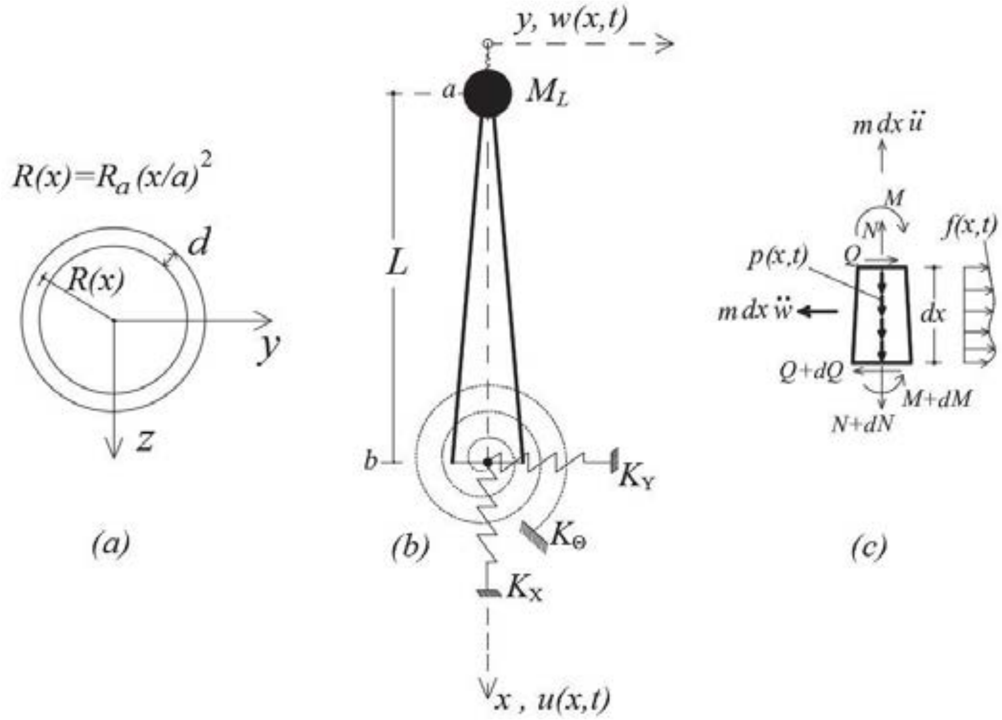

Figure 1. Cantilevered pylon with (a) ring cross-section of variable radius R; (b) length L with added mass and springs at the ends and (c) the free body diagram.

$$\frac{\partial}{\partial x}\left(EA(x)\frac{\partial u(x,t)}{\partial x}\right)-\frac{\partial}{\partial x}\left[Q(x,t)\frac{\partial w(x,t)}{\partial x}\right]-m(x)\frac{\partial^2 u(x,t)}{\partial t^2}=p(x,t) \quad (1a)$$

$$\frac{\partial^2}{\partial x^2}\left(EI(x)\frac{\partial^2 w(x,t)}{\partial x^2}\right)-\frac{\partial}{\partial x}\left[N(x,t)\frac{\partial w(x,t)}{\partial x}\right]+m(x)\frac{\partial^2 w(x,t)}{\partial t^2}=f(x,t) \quad (1b)$$

In the above, $u(x,t)$ and $w(x,t)$ are the axial and transverse displacements, respectively and $m(x)$ is the distributed mass. Next, the axial force, bending moment and shear force are defined as $N = EA(x)(\partial u/\partial x)$, $M = -EI(x)(\partial w^2/\partial x^2)$ and $Q = -E\frac{\partial}{\partial x}((I(x)\ \partial w^2/\partial x^2))$. Initial conditions are assumed to be zero, and three sets of boundary conditions are considered, which respectively address the fixed base case, the fixed base case with a lumped mass at the top, and the base isolated case:

$M(a,t) = Q(a,t) = N(a,t) = 0$ and $w(b,t) = \partial w(b,t)/\partial x = u(b,t) = 0$ (2a)

$M(a,t) = 0, Q(a,t) = M_L\ddot{w}(a,t), N(a,t) = M_L\ddot{u}(a,t)$ and
$w(b,t) = \partial w(b,t)/\partial x = u(b,t) = 0$ (2b)

$M(a,t) = Q(a,t) = N(a,t) = 0$ and
$M(b,t) = -K_\Theta \partial w(b,t)/\partial x,\ Q(b,t) = -K_Y w(b,t),\ N(b,t) = -K_X u(b,t)$ (2c)

In the above., $x = a$ is the top and $x = b$ is the base of the cantilevered pylon with length $L = b - a$. The lumped mass M_L placed at the top influences both axial and flexural vibrations, whereas the base springs K_X, K_Y, K_Θ respectively influence the longitudinal motion, the transverse motion and the base rotation.

2.1 Harmonic vibrations

By ignoring the coupling terms $\frac{\partial}{\partial x}\left[Q\frac{\partial w}{\partial x}\right]$ and $\frac{\partial}{\partial x}\left[N\frac{\partial w}{\partial x}\right]$ for the range of frequencies considered in here, and by differentiating the variable stiffness terms, we recover the following equations:

$$EA(x)u'' + \left[\frac{\partial EA(x)}{\partial x}\right]u' - m(x)\ddot{u} = -p(x,t) \tag{3a}$$

$$EI(x)w'''' + 2\left[\frac{\partial EI(x)}{\partial x}\right]w''' + \left[\frac{\partial^2 EI(x)}{\partial x^2}\right]w'' + m(x)\ddot{w} = f(x,t) \tag{3b}$$

In the above, $EA(x)$ and $EI(x)$ are the aggregate axial and flexural stiffness that varies along the pylon length $a \le x \le b$. The notation introduced now involves primes $(')$ and dots $(\cdot)$ to denote differentiation with respect to the spatial coordinate *x* and time *t*.

We now consider a slender, circular cylindrical pylon with a cross-section in the form of an annulus of constant thickness d and variable radius $R(x)$, which is a rather common design for pylons. The reference radius is the mean radius of the cross-section defined as $R = R_{ext} - d/2$, where R_{ext} is the external radius, see Fig. 1. For small thickness d, the cross-section area, moment of inertia and polar moment of inertia are closely approximated as $A = 2\pi dR,\ I = \pi R^3 d, J = 2I$, while the mass per unit length is $m = \rho A$. We adopt a general representation of a radius that changes quadratically with height, i.e. $R(x) = R_a \cdot (x/a)^2$, with R_a the mean radius at the top. Then, the following expressions for the pylon stiffness and mass are recovered:

$$EA(x) = (EA)_0\left(\frac{x}{a}\right)^2,\ EI(x) = (EI)_0\left(\frac{x}{a}\right)^6,\ m(x) = m_0\left(\frac{x}{a}\right)^2 \tag{4}$$

where $(EA)_0, (EI)_0, m_0$ are reference values computed at the top, i.e. for $R(x = a) = R_a$. Note that it is possible to handle material properties that are also position dependent, so long as the aggregate stiffness and mass values obey Eq. (4). We finally note in passing that torsional vibrations are of minor importance as ambient ground vibrations are unlikely to elicit torsion at the base of the shaft.

Assuming a time harmonic environment, the input and the response can be written in terms of position dependent amplitudes times the exponential term $\exp(i\omega t), i = \sqrt{-1}$, where $\omega\ (rad/s)$ is the frequency of vibration. Therefore, the dependent variables are now the amplitudes of the axial and flexural vibration $W(x), U(x)$ and we also define the corresponding amplitude of the external distributed forces as $F(x), P(x)$. The governing equations for harmonic motion are now

$$[x^2U'' + 2xU'] + \omega^2 m_0\left(\frac{x}{a}\right)^2\frac{a^2}{(EA)_0}U = -\frac{a^2}{(EA)_0}\cdot P(x) \tag{5a}$$

$$[x^6W'''' + 12x^5W''' + 30x^4W''] - \omega^2 m_0\left(\frac{x}{a}\right)^2\frac{a^6}{(EI)_0}W = \frac{a^6}{(EI)_0}\cdot F(x) \tag{5b}$$

which respectively are a Bessel equation of fractional order for the axial motion and Euler's equation for the flexural motion.

3. SOLUTIONS FOR LONGITUDINAL AND TRANSVERSE VIBRATIONS

To recover analytical solutions to the above equations, we first derive the homogeneous solution and then solve for the eigenvalue problem to recover the eigenproperties of the pylon, first for axial and then for flexural vibrations. The general form of the homogeneous solutions to Eq. (5) in the frequency domain are

$$U(x) = x^{-\frac{1}{2}} \cdot \{A_1 J_{\left(-\frac{1}{2}\right)}(\alpha x) + A_2 J_{\left(+\frac{1}{2}\right)}(\alpha x)\}, \;\; x > 0 \tag{6a}$$

$$W(x) = B_1|x|^{r_1} + B_2|x|^{r_2} + B_3|x|^{r_3} + B_4|x|^{r_4} \tag{6b}$$

In the above, $J_{(q)}$ are the Bessel functions of first kind and fractional order q, while exponents r_i, $i = 1{,}4$ are non-repeated complex numbers. Also, A_i,B_i are constants of integration to be determined from the boundary conditions.

For flexural vibrations, Euler's equation (5b) requires a preliminary transformation of variables as $x = e^y, y = \ln(x)$ to convert it into a differential equation with constant coefficients. The characteristic polynomial for this differential equation that must be solved for determining the exponents r_i is $r^4 + 6r^3 + 5r^2 - 12r - \beta^4 = 0$. Solution to the aforementioned quartic polynomial yields complex roots in the form $B_j x^{r_j} = B_j x^{a_j + ib_j} = B_j x^{a_j}\{\cos(b_j x) + \mathrm{i}\sin(b_j x)\}$, $i = \sqrt{-1}$. In our case,

$$r_1 = -\frac{3}{2} + \frac{\sqrt{(17 + 4\sqrt{(4+\beta^4)})}}{2}, r_2 = -\frac{3}{2} - \frac{\sqrt{(17 + 4\sqrt{(4+\beta^4)})}}{2}$$

$$r_3 = -\frac{3}{2} + i\frac{\sqrt{(4\sqrt{(4+\beta^4)} - 17)}}{2}, r_4 = -\frac{3}{2} - i\frac{\sqrt{(4\sqrt{(4+\beta^4)} - 17)}}{2}$$

with $W(\xi) =$

$$= \xi^{-\frac{3}{2}}\left(B_1 \xi^{\frac{\sqrt{(k+17)}}{2}} + B_2 \xi^{-\frac{\sqrt{(k+17)}}{2}} + B_3 \sin\left(\frac{\sqrt{(k-17)}}{2} \ln\xi\right) + B_4 \cos\left(\frac{\sqrt{(k-17)}}{2} \ln\xi\right)\right) \tag{7}$$

where $k = 4\sqrt{(\beta^4 + 4)}$ and for a dimensionless spatial parameter $\xi \in [1, b/a]$.

We adopt the Kelvin solid model with a complex elasticity modulus in the form $E^* = E(1 + i\delta), \delta = \eta\omega/2E$, where E is the original real-valued elasticity modulus and η is a constant in the viscoelastic stress-strain law. For concrete, the dimensionless damping coefficient δ values have been experimentally determined to range as $1\% - 5\%$, values which respectively correspond to pre-stressed and to weathered concrete. This complex number representation of the elastic modulus filters into the pressure and shear wave speeds c_p, c_S, and into the wave numbers for axial and flexural vibrations.

If tapering is ignored and the pylon cross-section is uniform with radius R_a, then the above homogeneous solutions reduce to

$$U(x) = A_1 \cos(\alpha x) + A_2 \sin(\alpha x), \alpha^2 = \omega^2/c_p^2 \tag{8a}$$

$$W(x) = B_1 \cos(\beta x) + B_2 \sin(\beta x) + B_3 \cosh(\beta x) + B_4 \sinh(\beta x), \beta^4 = \omega^2 \frac{\rho A_0}{E I_0} \tag{8b}$$

3.1 The eigenvalue problem

The eigenvalue problem derives from imposing homogeneous boundary conditions, see Eq. (2a). The boundary conditions corresponding to the lumped mass and the elastic springs can be rendered homogeneous as well, leading to a more complicated solution for the eigenfunctions $\Phi_n(x), n = 1,2, \dots \infty$. The corresponding eigenvalues $f_n\ (Hz)$ are recovered during this process by solving for the roots of a transcendental equation. More specifically, the solutions given in Eq. (6a) for axial vibrations and in Eq. (7) for flexural vibrations can be respectively recast in matrix form as

$$[G(\omega)]\{A\} = \{0\},\ [H(\omega)]\{B\} = \{0\} \tag{9}$$

respectively, with the former matrix size being $2x2$ and the latter being $4x4$. These matrices respectively contain Bessel functions and trigonometric functions evaluated at the two ends $x = a, b$ of the pylon. By setting the matrix determinants equal to zero and solving for the roots of resulting transcendental equations using the Newton-Raphson method, the eigenvalues of the pylon are recovered. Finally, the eigenfunctions are evaluated starting with a back-substitution of the eigenvalues in Eq. (9) and usually setting one of the coefficients of the vectors $\{A\}, \{B\}$ equal to one.

3.2 External loads

When external loads are present, one can opt to either employ modal analysis or to find a particular solution for the right-hand sides (*RHS*) of Eq. (5) corresponding to time harmonic forces, in which case the complete solution is the addition of the homogeneous and particular parts. For ambient vibrations in the form of ground motion, a complication arises due to the fact that one must distinguish between the displacement of the cantilever relative to its base, and its total displacement which is the addition of both. The generic form of ground motion, be it in the vertical or horizontal directions, is $x_g(t) = x_{go} \exp(i\Omega t)$, where $X_{go}(m)$is a mean value for the ground displacements and $\Omega\ (rad/s)$ is the frequency of vibration. Assuming U, W are relative to the base, then the *RHS* of Eq. (1) are $f(x,t) = p(x,t) = m(x) \cdot \Omega^2 \cdot x_{go} \cdot exp(i\Omega t)$. Two frequency ranges are relevant to the pylons considered here due to the passage of high speed trains: *(i)* High frequency base accelerations in the vertical direction in the range $f = \Omega/2\pi = 100 - 200\ Hz$ that result from the train's wheels running across rails that have minor imperfections and *(ii)* low frequency base accelerations in the horizontal direction in the range $f = 20 - 40\ Hz$ as the train moves rapidly and generates forward travelling elastic waves in the soil.

3.3 Mass dampers and base springs

If the pylon has a lumped mass M_L at the top, one boundary condition for each of the axial and flexural vibrations involves the acceleration at $x = a$. In a steady-state environment, these acceleration amplitudes are $-\omega^2 U(x), -\omega^2 W(x)$, to which the amplitude of the base acceleration $\Omega^2 \cdot x_{go}$ must be added. This still allows for a reformulation of the boundary conditions of Eq. (2b) in the homogeneous form specified by Eq. (9). The boundary conditions of Eq. (2c) involving the base isolation springs K_X, K_Y, K_Θ are simpler to implement because they involve relative displacements. For the flexural vibration case, each of the translational and rotational springs are examined separately. Since the eigenvalue formulation matrix equations resulting from the imposition of the boundary conditions are complex, there is some economy in computation to be gained if their inversion is carried out in closed form. This is trivial for the $2x2$ matrix $G(\omega)$ that yields constants A_1, A_2. It becomes more involved for the $4x4$ matrix $H(\omega)$ that yields constants B_1, B_2, B_3, B_4, and we give as example in the Appendix the transcendental equation that yields the flexural eigenfrequencies for a lumped mass M_T at the top of the pylon.

4. EIGENPROPERTIES OF PYLONS WITH PASSIVE CONTROL DEVICES

Following the modal analysis approach previously discussed, we will focus on pylons with a uniform cross-section, as being the more general reference case.

4.1 Longitudinal vibrations

The transient axial displacement for the damped catilevered pylon is as follows:

$$u(x,t) = \{\sum_{n=1}^{\infty} b_n^* \; \Phi_n(x)\} \cdot (e^{i\omega t}) \quad (10a)$$

$$b_n^* = x_{g0} \; z^{*2} \cdot \int_0^L \Phi_n(x)dx / \{(k_n{}^2 - z^{*2}) \int_0^L \Phi_n^2(x)dx\} \quad (10b)$$

In the above, summation is over all $n = 1,2,\ldots\infty$ eigenmodes, while complex coefficient z^* has real and imaginary parts given by

$$Re(z^*) = \omega \sqrt{\frac{\rho}{E}\frac{1}{D}} \sqrt{\frac{D+1}{2}}, \; Im(z^*) = -\omega \sqrt{\frac{\rho}{E}\frac{1}{D}} \sqrt{\frac{D-1}{2}} \quad (11)$$

with $D = (1 + \delta^2)$. The eigenfunction is defined in the interval $0 \le x \le L$ as $\Phi_n(x) = \cos(k_n x)$.

If a lumped mass $M_L = R_M M_T$ is placed at the top of the pylon, the axial displacement is

$$u(x,t) = \{\sum_{n=1}^{\infty} b_n^* \; \Phi_n(x) + ax\} \cdot (e^{i\omega t}) \quad (12a)$$

$$b_n^* = x_{g0} z^{*2} \cdot \{\int_0^L \Phi_n(x)dx + a\int_0^L x\Phi_n(x)dx\} / \{(k_n{}^2 - z^{*2}) \int_0^L \Phi_n^2(x)dx\} \quad (12b)$$

with coefficient $a = \frac{x_{go}/L}{\{(\Gamma^2/\omega^2)-1\}}$, $\Gamma^2 = \frac{E^*}{\rho R_M L^2}$ and complex coefficient z^* given by Eq. (11).

4.2 Transverse vibrations

As in the above, reconstitution of the transverse displacement using modal analysis for the damped, flexible pylon with uniform cross-section is given as

$$w(x,t) = \{\sum_{n=1}^{\infty} b_n^* \; \Phi_n(x)\} e^{i\omega t}, \; b_n^* = \frac{x_g \; z^{*4} \int_0^L \Phi_n(x)dx}{(k_n{}^4 - z^{*4}) \int_0^L \Phi_n^2(x)dx} \quad (13)$$

with the real and imaginary parts of the complex coefficient z^* given as

$$Re(z^*) = \sqrt{\frac{\omega}{r}} \sqrt[\frac{1}{4}]{\frac{\rho}{E}} \sqrt{\frac{1}{2\sqrt{D}} + \frac{\sqrt{D+1}}{2\sqrt{2}D}}, \; Im(z^*) = -\sqrt{\frac{\omega}{r}} \sqrt[¼]{\frac{\rho}{E}} \sqrt{\frac{1}{2\sqrt{D}} - \frac{\sqrt{D+1}}{2\sqrt{2}D}} \quad (14)$$

and where $r = \sqrt{I/A}$ is the radius of gyration of the cross-section. The general form of the eigenfunctions is

$$\Phi_n(x) = \sin(k_n x) + \sinh(k_n x) + C_n * (\cos(k_n x) + \cosh(k_n x)) \quad (15)$$

When a horizontal base spring K_Y is placed at the pylon's base, then constants C_n appearing in the eigenfunctions are given below as

$$C_n = \frac{\sin(k_n L) + \sinh(k_n L) - (EI/K_Y) \cdot k_n^3 \cdot (-\cos(k_n L) + \cosh(k_n L))}{-(\cos(k_n L) + \cosh(k_n L)) + (EI/K_Y) \cdot k_n^3 \cdot (\sin(k_n L) + \sinh(k_n L))} \quad (16)$$

Next, when a rotational spring K_Θ is placed at the base, the new constants C_n are now

$$C_n = \frac{\cos(k_n L) + \cosh(k_n L) + (EI/K_\Theta) \cdot k_n \cdot (-\sin(k_n L) + \sinh(k_n L))}{-(-\sin(k_n L) + \sinh(k_n L)) - (EI/K_\Theta) \cdot k_n \cdot (-\cos(k_n L) + \cosh(k_n L))} \quad (17)$$

5. NUMERICAL STUDIES FOR A FLEXIBLE PYLON

The aim here is to derive transmissibility (*TR*) functions for both axial and flexural vibrations of a cantilevered pylon serving as part of the network for electrified railway lines. The pylon material is pre-stressed concrete, and the relevant geometric and mechanical properties are given in Table 1 below, including M_T, the total mass of the pylon. All subsequent computations were carried out in a Python programming environment [11], where computation times did not exceed $8\ sec$ for the *TR* functions that follow, which are parametric in the mass ratio $R_M = M_L/M_T$ and in the spring K_X, K_Y, K_Θ constants.

a (m)	*b(m)*	*d (m)*	*R(a) (m)*	*R(b) (m)*
39.5	*49.5*	*0.0875*	*0.215*	*0.3375*

E (kPa)	*ρ (tn/m³)*	*m_0 (tn/m)*	*M_T (tn)*	*δ (%)*
$44.4 \cdot 10^6$	*2.55*	*0.301*	*3.84*	*5.0*

Table 1: Properties of the pre-stressed R/C cantilevered pylon

5.1 Preliminary calculations

We define an equivalent, uniform cantilevered pylon that has a constant cross-section defined by the base radius $R(b)$ through-out its height. This is simply done for comparison purposes with the tapered one, and Table 2 lists the first three axial and flexural eigenfrequencies for both types of pylons. We observe that the difference in the first fundamental frequency of the pylon is in the neighborhood of *5%* between the tapered and the uniform cross-section variants. Further such comparison studies can be found in Ref. [4].

Pylon type	*f_1 (Hz) axial*	*f_2 (Hz) axial*	*f_3 (Hz) axial*	*f_1 (Hz) flexural*	*f_2 (Hz) flexural*	*f_3 (Hz) flexural*
Uniform	*104.3*	*312.9*	*521.6*	*5.57*	*34.92*	*97.78*
Tapered	*114.0*	*316.5*	*523.7*	*5.84*	*30.47*	*80.85*

Table 2: Comparison of the eigenvalues between R/C pylon uniform and tapered cross section.

5.2 The eigenvalue problem for a base-isolated pylon with a uniform cross-section

For illustrative purposes, Fig. 2 below shows the pylon's first three flexural eigenmodes for the case of a translational spring K_Y whose value increases so that in Fig. 2(c) the fixed-base pylon case is recovered.

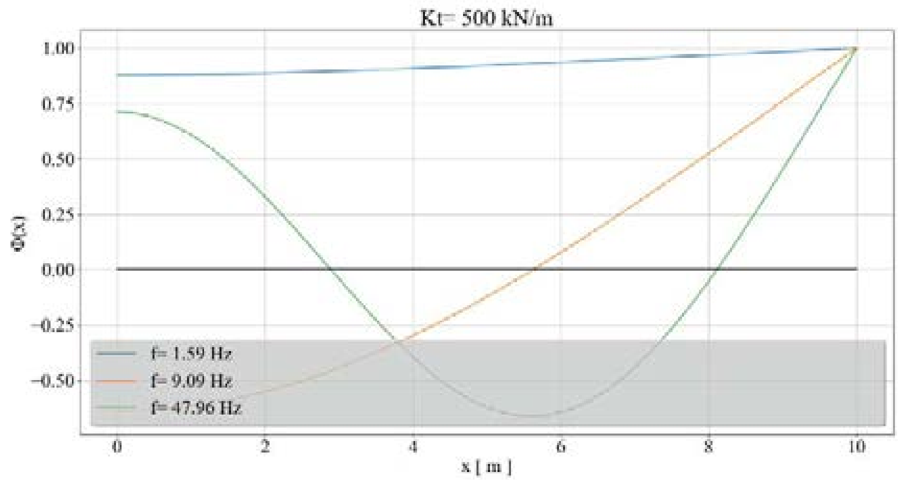

(a)

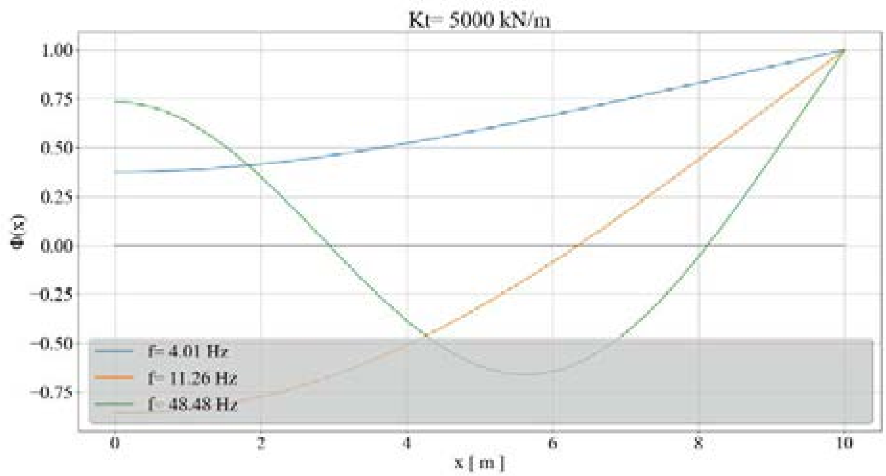

(b)

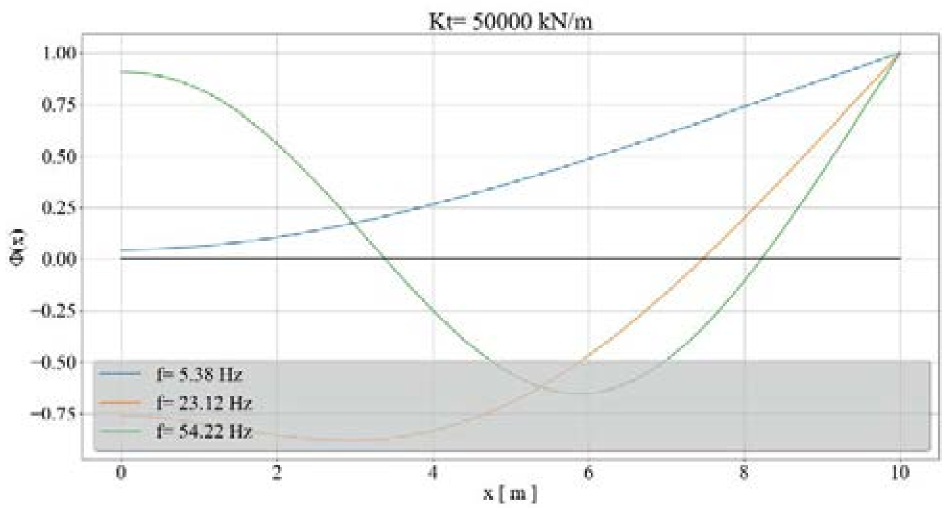

(c)

Figure 2: First three eigenfrequencies and eigenfuntions of a flexible pylon under transverse vibrations as a function of the translational base spring magnitude: (a) Soft spring, $K_Y=500$ *kN/m*, (b) intermediate spring, $K_Y=5{,}000$ *kN/m* and (c) stiff spring $K_Y=50{,}000$ *kN/m*.

Also, Fig. 3 is a convergence study on how the first three flexural eigenfrequencies of the base isolated pylon converge to the values for the fixed-base case as the magnitude of the translational and rotational base springs increases

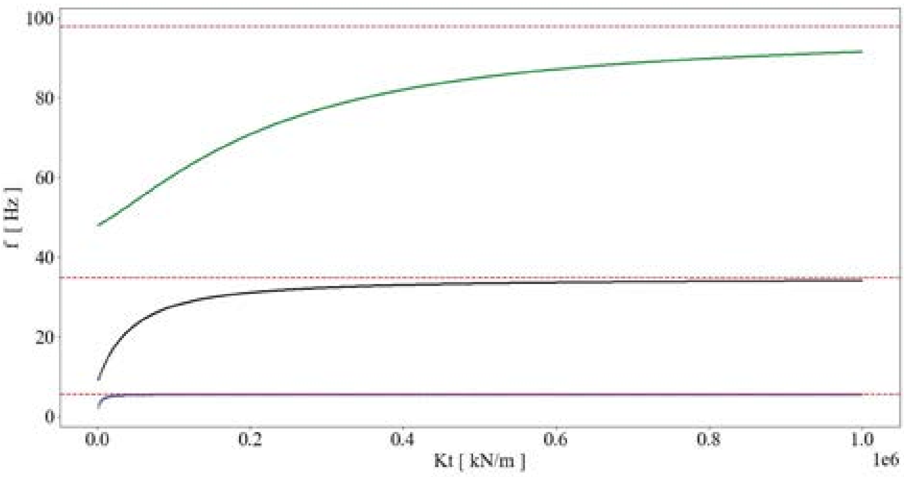

(a)

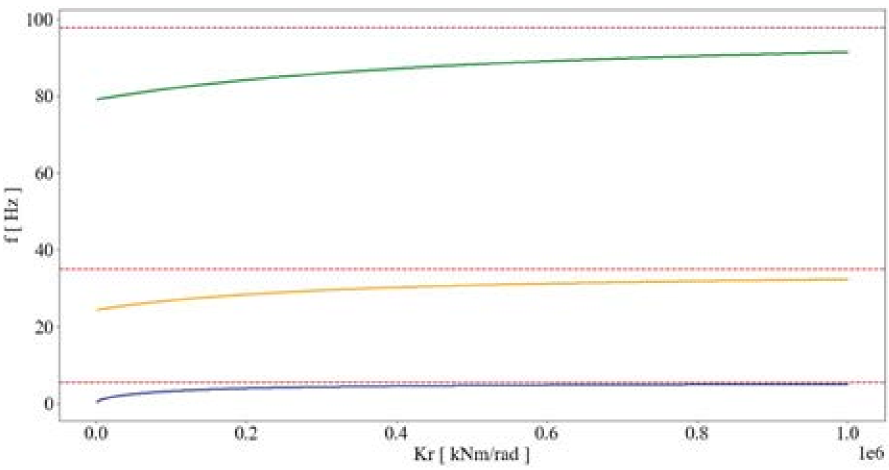

(b)

Figure 3: Convergence study on the first three flexural eigenfrequencies of the base-isolated pylon as a function of spring stiffness: (a) translational spring K_Y and (b) rotational spring K_Θ. Note: The dotted red line is for the fixed-base pylon.

5.3 Transmissibility functions for longitudinal vibrations

We next proceed to recover *TR* functions for the reference case of the equivalent uniform pylon, keeping in mind that tapering basically acts as a perturbation of the first eigenfrequencies of an equivalent pylon with a uniform cross-section. Since the eigenfrequencies of pylons are widely spaced, we resort to *log-log* plots. Starting with Fig. 4, we observe that until the first axial eigenfrequency is reached, the presence of the lumped mass at the top is of minor consequence, but still somewhat detrimental. However, as the frequency continues to go up, the lumped mass starts actively reducing the motion by as much as an order of magnitude, and even a small mass of 10% of M_T is effective. Note here the emergence of a new eigenfrequency, otherwise absent when there is no top mass. The situation with the vertical base spring is quite different, because at low frequencies, below the first eigenfrequency, we have substantial decrease in the *TR* values as compared to the fixed base, which roughly corresponds to the spring with the largest values, namely $K_X=5\cdot10^6$ *kN/m* . As the frequency goes up, the *TR* exhibit minor fluctuations but the motion de-amplification is still substantial.

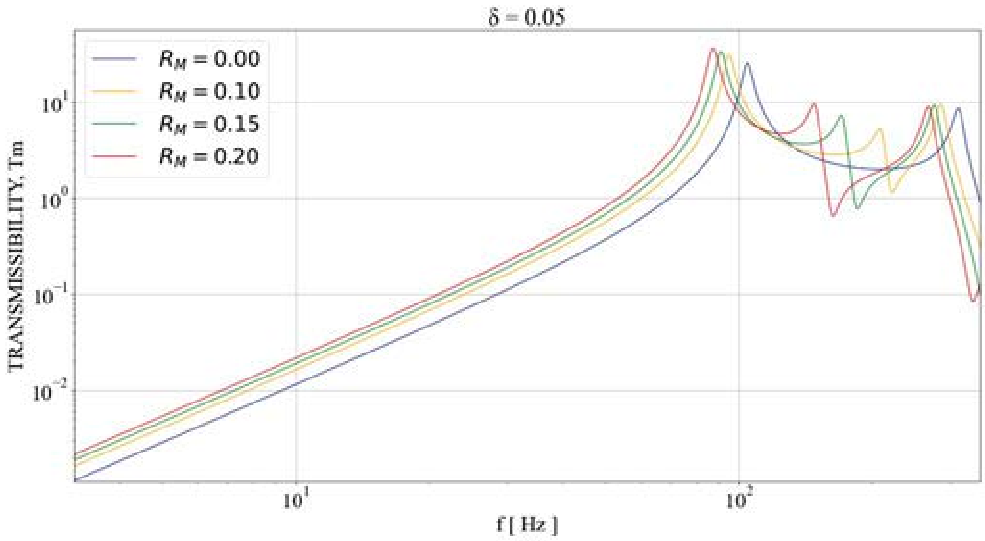

(a)

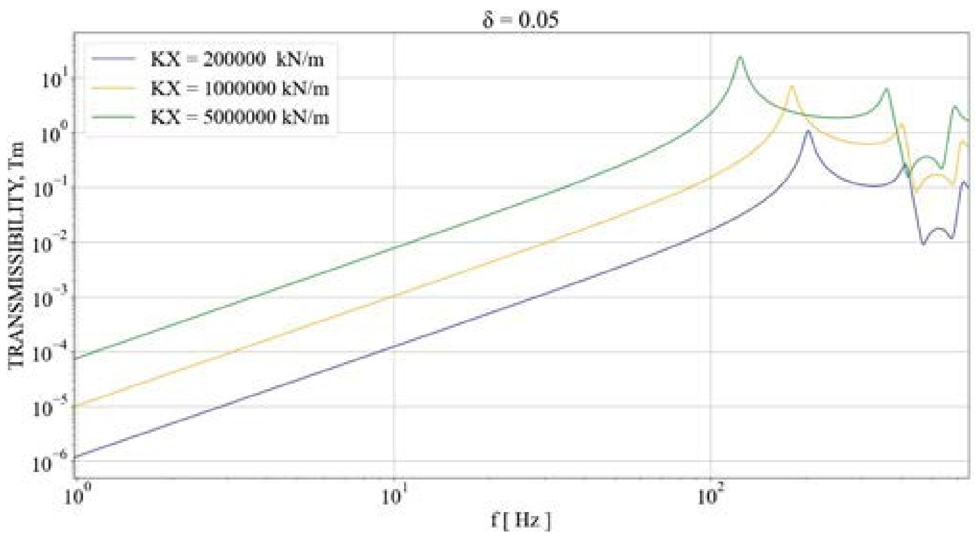

(b)

Figure 4: Transmissibility functions *TR* between top and ground displacement amplitudes versus frequency *f* for longitudinal pylon vibrations under a normalized sinusoidal ground acceleration input and for a damping *δ* value of *5%* as a function of: (a) mass ratio $R_M=M_L/M_T$; (b) vertical base spring K_X values.

5.4 Transmissibility functions for transverse vibrations

We continue with Fig. 5 for flexural vibrations, where the *TR* functions for the base isolation springs present a rather complicated situation. Assuming that the highest spring values approach the fixed-base case, then base isolation springs are ineffective at low frequencies, i.e. those below the first flexural eigenfrequency. As we move past that value, only the horizontal spring is effective in producing de-amplification of motion. Finally, the rotational spring remains ineffective at both the low and high ends of the frequency spectrum, where it shifts the fixed-base dominant eigenfrequency to lower values. It is effective only when the external frequency of vibration approaches a narrow frequency range around the fixed-base pylon eigenfrequencies.

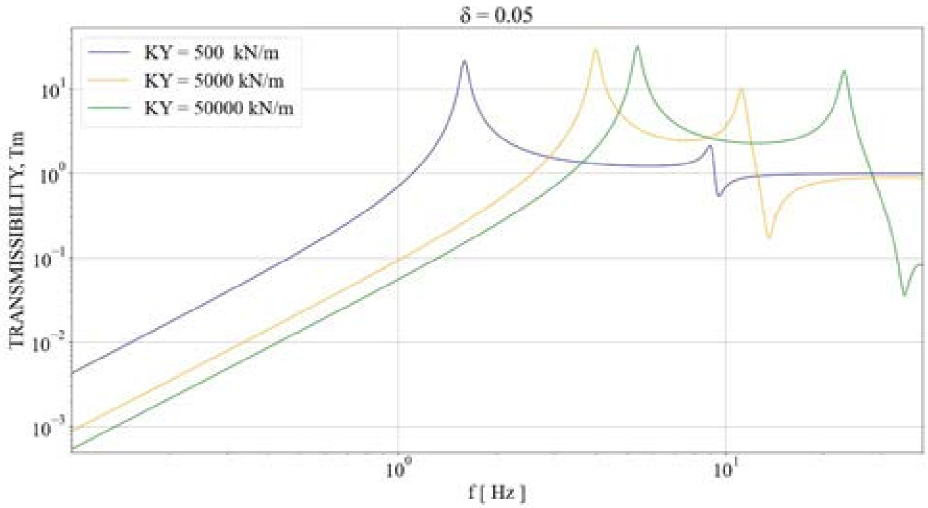

(a)

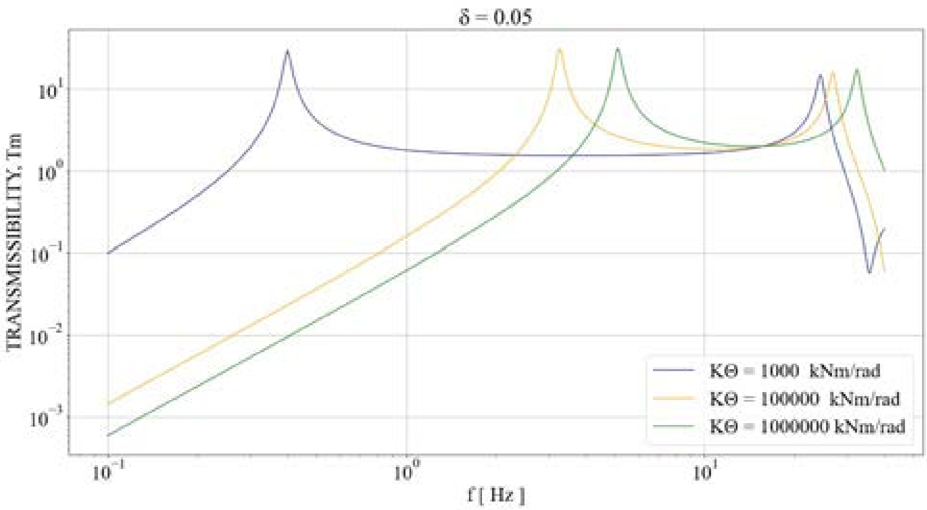

(b)

Figure 5: Figure 4: Transmissibility functions *TR* between top and ground displacement amplitudes versus frequency *f* for transverse pylon vibrations under a normalized sinusoidal ground acceleration input and for a damping *δ* value of *5%* as a function of: (a) horizontal base spring K_Y values and (b) rotational base spring K_Θ values.

6. CONCLUSIONS

In this work, we have derived solutions for the transmission of motion between the top and base of a cantilevered pylon, to which either a lumped mass is attached at the top or springs are inserted at the base for the purpose of acting as passive control devices. Of course, it may be that a lumped mass is already attached to the pylon, as would for lighting devices, cable supports, signal transmission apparatus, etc., which implies that the results generated here are still applicable. The same holds true if the pylon is founded on soft soil, in which case we have soil-structure-interaction phenomena and the ground is replaced by an equivalent set of springs.

For a typical R/C pylon used in electric rail lines, with vibrations induced by passing trains in both the vertical direction and on the horizontal plane, the presence of the lumped mass at the top of the pylon is beneficial in the high frequency range, where we see an amplitude reduction in the pylon displacements. Conversely, in the low frequency range as compared to the pylon fundamental eigenfrequency, the presence of a lumped mass ranges is of minor significance and may even be detrimental. Similar conclusions can be drawn in reference to the presence of base isolation springs that become effective in the higher frequency range. In the low frequency range, however, their presence is detrimental, as they result in an increase in amplitude at the top for transverse vibrations, but beneficial for longitudinal vibrations.

The presence of a lumped mass and of base isolation springs becomes important when viewed in terms of SHM, because these passive damping mechanisms can be upgraded to a semi-active status [9]. For instance, it may be possible to allow for the lumped mass to fluctuate as the pylon structural vibrations unfold with time, provided a suitable mechanism can be added for this purpose. In addition, there would have to be a control algorithm, as for instance a predictor-corrector method that computes the imminent displacement at the top of the pylon and energizes the mechanism if this displacement exceeds a prescribed limit. A similar situation can be envisaged for the case of a base isolation mechanism. In both cases, the use of control algorithms pre-supposes the existence of robust and efficient structural analysis capabilities, as would be the case for the analytical solutions presented herein.

Acknowledgement: The authors acknowledge support from the German Research Foundation (DFG) projects SM 281/14-1 entitled “Data-driven analysis models for slender structures using explainable artificial intelligence” and SM 281/20-1 entitled "Resilient infrastructure based on cognitive buildings", Prof. K. Smarsly, University of Hamburg-Harburg, coordinator.

REFERENCES

[1] K.F. Graff, *Wave motion in elastic solids*, Ohio State University Press, 1975.

[2] E. Kausel, *Advanced structural dynamics*, Cambridge University Press, 2017.

[3] I. Elishakoff, J. Kaplunov, E. Nolde, Celebrating the centenary of Timoshenko’s study of effects of shear deformation and rotatory inertia, *Applied Mechanics Reviews of ASME*, **67**, 060802-1, 2015.

[4] G.D. Manolis, G. I. Dadoulis, S.I. Pardalopoulos, K. Dragos, Analytical models for the monitoring of flexible antennas under environmentally induced dynamic loads, *Acta Mechanica,* **231**, 3621-3624, 2020.

[5] J.C. Snowdon, *Vibration and shock in damped mechanical systems*, J. Wiley, 1968.

[6] C.C. Chaves-Júnior, R.F. de Alencar Araujo, C.M.C. de Souza, A.C.A. Ferreira, P.M.V. Ribeiro, A collocation method for bending, torsional and axial vibrations of offshore wind turbines on monopile foundations, *Ocean Engineering*, **217**, 107735, 2020.

[7] S. Nagarajaiah, S. Dyke, J.P. Lynch, A. Smyth, A. Agrawal, M. Symans and E. Johnson, Current directions of structural health monitoring and control in USA. *Advances in Science and Technology*, **56**, 277-286, 2008.

[8] C.R. Farrar and K. Worden. *Structural health monitoring: A machine learning perspective*. J. Wiley, 2012.

[9] K. Smarsly and K.H. Law, A migration-based approach towards resource-efficient wireless structural health monitoring. *Advanced Engineering Informatics*, **27:4**, 625-635, 2013.

[10] S. I. Pardalopoulos, G. D. Manolis, An engineering approach for evaluating the dynamic response of acceleration-sensitive secondary systems in flexible structures, *Earthquake Engineering and Structural Dynamics*, 2021. https://doi.org.10.1002/eqe.3438

[11] *Python Software Foundation*, Beaverton, Oregon, USA, 2001. *www.python.org*

APPENDIX

We derive here the transcendental equation for flexural vibrations of a tapered pylon with a lumped mass M_L at the top, whose numerical solution by the Newton-Raphson method yields the eigenfrequencies. This derivation assumes that this mass is activated by the relative transverse motion $w(x,t)$ of the pylon, which is the case that appears often in the literature. We should note, however, that the mass is influenced by the total motion that includes the base motion $x_g(t)$. Finally, recovery of the first three eigenmodes is usually deemed sufficient for any subsequent dynamic analysis. More specifically, we start with the shear force boundary condition

$$Q(a,t) = M_L\ddot{w}(a,t) \Rightarrow -EI'(a)w''(a,t) - EI(a)w'''(a,t) = M_L\ddot{w}(a,t)$$

We follow with a substitution for $w(x,t)$ in terms of the generalized coordinates $q(t)$ and the eigenfunctions $\Phi(x)$:

$$-EI'(a)W''(a)q(t) - EI(a)W'''(a)q(t) = M_L W(a)\ddot{q}(t)$$

However, the generalized coordinates obey the single degree-of-freedom equation as

$$\ddot{q}(t) + \omega^2 q(t) = 0 \Rightarrow \ddot{q}(t) = -\omega^2 q(t)$$

Since the bending moment at the pylon's top is zero, we have that $M(a) = 0 \Rightarrow \Phi''(a) = 0$. Manipulation of the boundary condition equation yields

$$-EI(a)W'''(a)q(t) = M_L W(a)\ddot{q}(t) = M_L W(a)(-\omega^2)q(t) \Rightarrow$$
$$EI(a)W'''(a) = M_L W(a)\omega^2$$

Next, we use the dimensionless length $\xi = \frac{x}{a}, \xi \in [1, b/a]$ and of moment of inertia of the tapered pylon $I = I_O(x/a)^6 = I_O\xi^6$ to recover the following equation:

$$EI_O\Phi'''(1)/a^3 = M_L W(1)\omega^2 \quad \text{(A.1)}$$

The total mass of the pylon M_T is then computed as

$$M_T = \int_{x=a}^{x=b} \rho\, 2\pi d R_O \left(\frac{x}{a}\right)^2 dx = \int_{\xi=b/a}^{\xi=1} \rho\, 2\pi d R_O \xi^2 a d\xi = (2\pi R_O d)\frac{a}{3}\rho\left(\frac{b^3}{a^3}-1\right) =$$

$$= A_O \frac{a}{3}\rho\left(\frac{b^3}{a^3}-1\right) = \rho A_O \Lambda,$$ where $\Lambda = \frac{a}{3}\left(\frac{b^3}{a^3}-1\right)$, $R = \frac{M_L}{M_T}$, and $\beta^4 = \frac{\rho A_O a^4}{EI_O}\omega^2$.

By inserting the above expressions in Eq. (A.1) we recover that

$$-\left(\frac{M_L}{\rho A_O \Lambda}\right)\left(\frac{\omega^2 \rho A_O a^4}{EI_O}\right)\frac{\Lambda}{a}W(1) + W'''(1) = -R\cdot\beta^4\cdot\left(\frac{\Lambda}{a}\right)\cdot W(1) + W'''(1) = 0$$

We now introduce the homogeneous solution for flexural vibrations as

$$W(\xi) = \xi^{-\frac{3}{2}}\{B_1\xi^{\frac{\sqrt{(k+17)}}{2}} + B_2\xi^{-\frac{\sqrt{(k+17)}}{2}} + B_3 sin\left(\frac{\sqrt{(k-17)}}{2}ln\xi\right) + B_4 cos\left(\frac{\sqrt{(k-17)}}{2}ln\xi\right)\}$$

where $k = 4\sqrt{(\beta^4+4)}$. Now we can define the following quantities:

$$A_1(\xi) = \xi^{\frac{-3}{2}}\xi^{\frac{\sqrt{(k+17)}}{2}}, A_2(\xi) = \xi^{\frac{-3}{2}}\xi^{\frac{-\sqrt{(k+17)}}{2}},$$

$$A_3(\xi) = \xi^{\frac{-3}{2}}\sin\left\{\frac{\sqrt{(k-17)}}{2}ln(\xi)\right\},\ A_4(\xi) = \xi^{\frac{-3}{2}}\cos\left\{\frac{\sqrt{(k-17)}}{2}ln(\xi)\right\}$$

The full set of boundary conditions for the lumped mass at the top is

$$W(b/a) = 0, W'(b/a) = 0, W''(1) = 0, -R\cdot\beta^4\cdot\Lambda\cdot a^{-1}\cdot W(1) + W'''(1) = 0$$

Finally, to recover the wave numbers, the determinant of the $4x4$ matrix is set equal to zero:

$$det = \begin{bmatrix} \alpha_1 & \alpha_2 & \alpha_3 & \alpha_4 \\ \beta_1 & \beta_2 & \beta_3 & \beta_4 \\ \gamma_1 & \gamma_2 & \gamma_3 & \gamma_4 \\ \delta_1 & \delta_2 & \delta_3 & \delta_4 \end{bmatrix} = 0 \qquad \text{(A.2)}$$

The matrix terms appearing in Eq. (A.2) are as follows:

$$\alpha_1 = A_1(b/a), \alpha_2 = A_2(b/a), \alpha_3 = A_3(b/a), \alpha_4 = A_4(b/a)$$
$$\beta_1 = A_1'(b/a), \beta_2 = A_2'(b/a), \beta_3 = A_3'(b/a), \beta_4 = A_4'(b/a)$$
$$\gamma_1 = A_1''(1), \gamma_2 = A_2''(1), \gamma_3 = A_3''(1), \gamma_4 = A_4''(1)$$
$$\delta_1 = -R\left(\frac{k^2}{16}-4\right)\cdot\left(\frac{\Lambda}{a}\right)A_1(1) + A_1'''(1), \delta_2 = -R\left(\frac{k^2}{16}-4\right)\cdot\left(\frac{\Lambda}{a}\right)A_2(1) + A_2'''(1)$$
$$\delta_3 = -R\left(\frac{k^2}{16}-4\right)\cdot\left(\frac{\Lambda}{a}\right)A_3(1) + A_3'''(1), \delta_4 = -R\left(\frac{k^2}{16}-4\right)\cdot\left(\frac{\Lambda}{a}\right)A_4(1) + A_4'''(1)$$